

Float: Spherical Ball, Frame: Wooden, Electromagnet: Cylindrical, Core: Soft iron.

The Dimension of the frame is given by: height: 160 mm, width: 40 mm, length: 80 mm and thickness of wood: 10 mm.

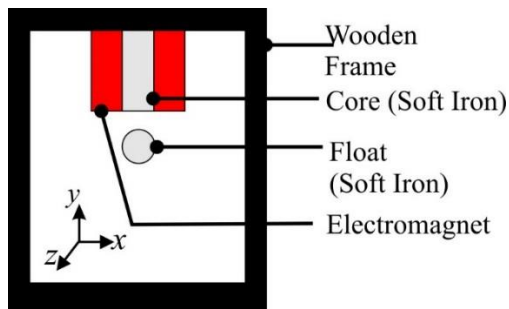


Figure 1: Schematic diagram of the first model.

Dimension of the spherical float is taken as follows:

Let the designed force generation by electromagnet to lift the float = 0.49N, material: Soft Iron AISI 1008 (for high magnetic permeability), density of AISI 1008, $\rho = 7872 \text{ kg/m}^3$, the acceleration of gravity, $g = 9.8 \text{ ms}^{-2}$ And also, Spherical float radius: 11mm, Spherical ball mass: 43.77 grams (approx.), Core Material: Ferrite, Core diameter: 22 mm, Core height: 40 mm, Air gap: 1 mm.

To design the electromagnet theoretically the model was transformed to a magnetic circuit. Then some assumption was made to find out the ideal electromagnet.

The following assumptions were made:

1. The distance of the armature from the core is much smaller than the average linear dimension of the pole cross section of the electromagnet,
2. The magnetic field in the gap between the ball and the core is uniform.
3. There is no magnetic flux leakage.

To design the electromagnet firstly we need to determine the flow for a required magnetic induction.

Here, P = Magnetic pressure, B = Magnetic flux density/ Magnetic induction, H = Magnetic field strength in amperes/meter, μ = Absolute permeability, μ_0 = Permittivity of air, A = Cross sectional area of the ball and core in square meters, F = Force on the ball in newton, Φ = Magnetic flux in Wb.

Magnetic Pressure created by the electromagnet on an object is given by

$$P = \frac{B^2}{2\mu_0} \text{ Pa. So, Force} = F = \frac{B^2 A}{2\mu_0} N$$

The magnetic induction remains constant to produce required force at 1 mm air gap. As the cross-sectional area of core and ball are the same.

$$H_{\text{air gap}} = \frac{B}{\mu_0} \text{ as, } B = \mu H. \text{ Float material AISI 1008 (ball material)}$$

Table 1: From B-H curve of iron material.

B	H
0.1828	107.92
0.1365	82.67

Source: Ansys Maxwell software B-H curve for AISI 1008.

From Table 1, for $B=0.140 \text{ T}$, $H(\text{ball})=84.57 \text{ amp/meter}$. Total magnetic voltage drop is given by $=\sum H_k l_k$. In the armature voltage drop $=H_{\text{float}} * 0.022 = 84.57 * 0.022 = 1.8605$

$$H_{\text{air gap}} = B_p / (\mu_0) = 111408 \text{ amp/meter, Magnetic voltage drop in air gap} = 0.001 * 111408 = 111.408 \text{ amp/m. Magnetic voltage drop in core} = 111.40 * 0.04 = 4.456$$

$$\text{Total magnetic voltage drop} = (4.456 + 111.40 + 1.8605) = 117.71$$

So, in ideal case, where all the assumptions hold, required Ampere turn = 117.71

$$\text{Current in the coil} = \frac{\text{Ampere-turn}}{\text{Number of turns}} = \frac{117.71}{400} = 0.29429 \text{ A}$$

From this mathematical analysis, it is clear that without any flux leakage only 117-120 ampere-turns of magnetomotive force is enough to lift 3N weight of soft iron float.

4. FIRST (NAIVE) DESIGN OF ELECTROMAGNETIC SUSPENSION SYSTEM (ESS)

In this first electromagnetic suspension system, the analysis is done with a magnetomotive force of 1900 ampere-turns at one mm distance to simulate the force on the float. With the configuration given at figure 1.

4.1. Result of simulation study and discussion (First Model)

In this magnetic circuit, the circuit is not closed. It is practically a straight line. As a result, there is a huge magnetic flux loss. This loss happens because the energy storage of free space is maximum. A lot of flux lines leaks from the open circuit as seen in Figure 3.

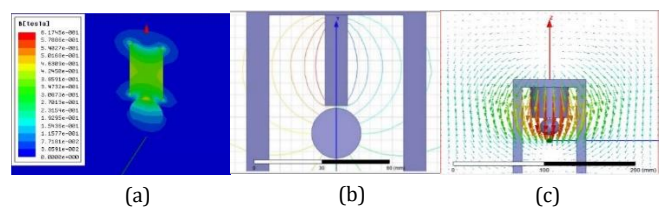


Figure 2: (a) Simulation result of magnetic flux density, (b) magnetic flux flow pattern of first model in 2D analysis, (c) vector distribution of magnetic flux

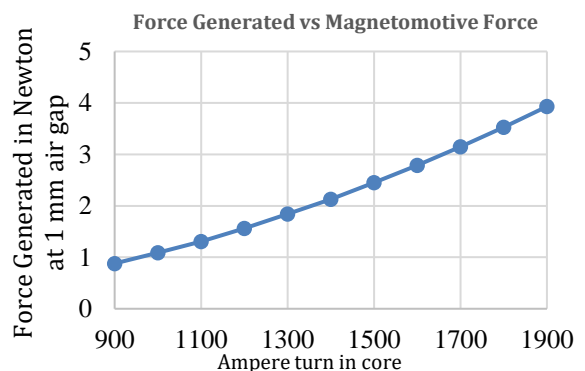


Figure 3: Variation of force on float for different excitation (First model) From the simulation result in Figure 3 it can be seen that for this type of electromagnet and wooden frame 1700 Ampere-turn will create 3N force at 1 mm separation distance from cylindrical core. The magnetic flux leakage can further be confirmed by the condition of B field vector in the region Figure 2(c).

Figure 4 represents the force vs gap distance data for cylindrical core, ball shaped float and wooden frame. From Figure 2(a) and Figure 2(c) it is obvious say that a large amount of power is lost in this arrangement. Thus due to high current flowing through the coil and the temperature of will be higher in this case. Also there may remain a possibility of saturation of core due to high current flow. These are some of the disadvantages which is not suitable to use when high amount of force is needed to be generated.

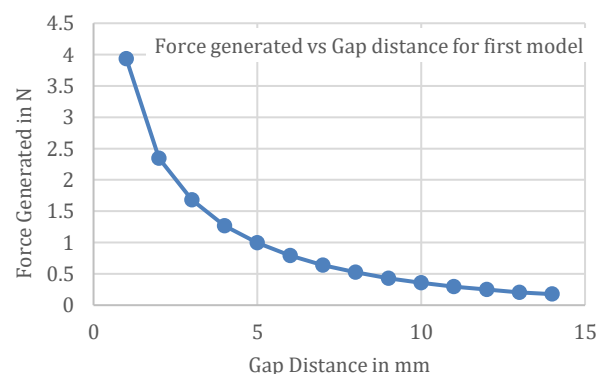


Figure 4: Variation of force on float at different air gap

The ampere-turn needed for this type of electromagnet if there is no flux leakage is calculated through theoretical analysis in previous section. and this result is compared with the simulated result to find out energy loss in this process.

The next portion of this discussion is continued with the focus of reduction of ampere-turns as much as possible. So, if this design can be improved to a design where the required ampere-turn is less then there are several advantages.

1. The current required in the coil will be less. So, the heat loss from coil will also reduce.
2. The operating cost will also be reduced.
3. The device will be able to operate longer period continuously.

5. DESIGN USING IRON FRAME

In practical scenario, there is a lot of flux leakage in model of Figure 1. One of the main reasons of the flux leakage here is that the frame is wooden and its relative permittivity is almost equal to 1. So, it has virtually no helpful effect in creating a closed magnetic circuit. So, we changed our frame to an iron frame. With this change the magnetic field in iron became saturated. The saturation flux density of soft iron can be found in a B-H curve. And its value is 1.6 Tesla. So, to keep the magnetic flux density within 1.6T to ensure that no saturation occurs the magnetomotive force was reduced to 150 amp-turns. This in turn reduces the magnetic flux density. Other than this all of our design remains the same.

5.1 Simulation result and discussion

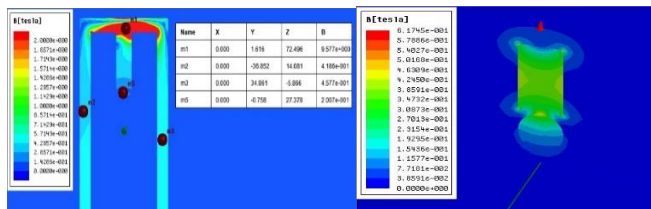


Figure 5: Comparison of simulation result between design with iron frame vs first design with wooden frame in respect of magnetic flux distribution.

In the above figure it can be seen that, a higher magnetic flux density is created in this frame. But the magnetic flux density around the float is negligible. And iron frame has trapped a significantly large amount of magnetic flux. For this reason, the force created on the float is negligible. And so, this design has been discarded. But problems of this design have been analyzed for further development purposes.

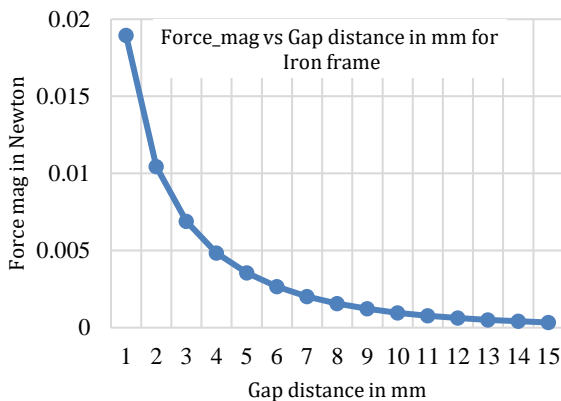


Figure 6: force generated on float in design with iron frame

Figure 6 shows the amount of force generated vs air gap distance for iron frame magnetic suspension system.

5.2 Problem of iron frame

The iron frame is directly attached to electromagnet. So, the iron frame gets saturated quickly even at low magnetomotive force (Amp-turns). Since iron is a very good conductor of magnetic flux. The saturation property of iron is found in B-H curve. The saturation occurs at steel at about 1.5T. This is a constraint posed by material property of steel. It shows it is not possible to increase the magnetomotive force (Amp-turns) indefinitely to get more flux density.

There is another drawback. And that is there is a large possibility of attraction of float towards iron frame. Which exerts an additional force on the float when it levitates. The flux line simulation for this condition is given in Figure 10. For these problems iron frame is not used in forthcoming designs. Neutral wooden frame has been preferred for these reasons.

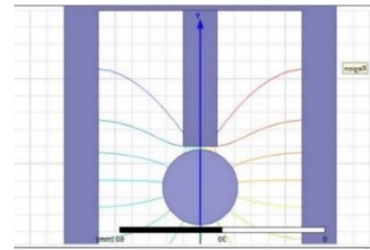


Figure 7: Magnetic flux flow pattern of improved design with iron frame in 2D analysis.

6. FURTHER IMPROVEMENT OF THE DESIGN BY CHANGING THE FLOAT SHAPE

Another improvement which can be done to increase the force on the float is by changing geometrical shape of float. From Figure 2(a) it can be concluded that for spherical float the B field cut by the float is stronger towards the electromagnet, and weaker away from it. Since the spherical ball has same geometry all around. Since with the increase in y axis distance the strength of B field fluctuates rapidly than other two dimensions. For this reason, spherical shape is not the best shape to retrieve more force from the electromagnetic field.

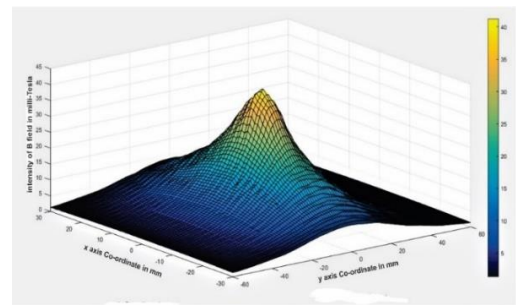


Figure 8: Variation of magnetic flux density at different position of x - z plane with constant air gap

The simulation result shown in Figure 8 and Figure 9 shows the magnitude of B field along different point of x - y plane (Figure 9) varies. From Figure 9 it can be seen that B field is maximum in a circular shape region. So, the geometry of improved float should have circular cross-section. It should also have small thickness in y direction. The geometry of the modified float is given in Figure 10. From the analysis, it seems that this shape should be able to pull greater weight for a given B field.

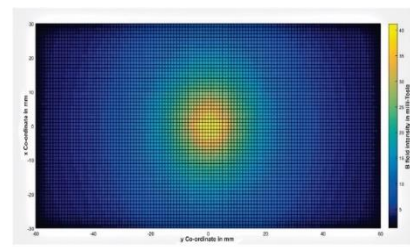


Figure 9: Projection of flux distribution on x - y plane

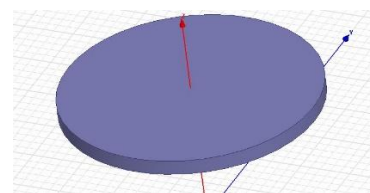


Figure 10: Modified float shape after analysis

6.1. Design of plate shaped float

Material: Iron AISI 1008

Let, D = 50 mm, so, h = 3.23 mm = 3 mm. Using these values, the mass of actual plate is 46.37 grams

6.2. Result of simulation study and discussion (Plate shape float and wood frame)

In Figure 12 the curve for plate shape float with wooden frame is given. It can be seen, with this arrangement the weight lifted is much greater to that found in the first naive design. From the simulation it was also found that the amount of flux cut is much higher than spherical ball.

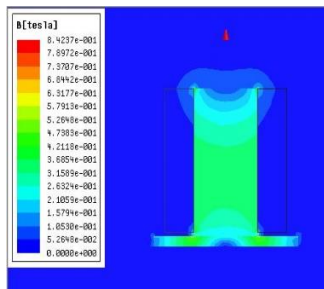


Figure 11: Magnetic flux distribution for plate shaped float

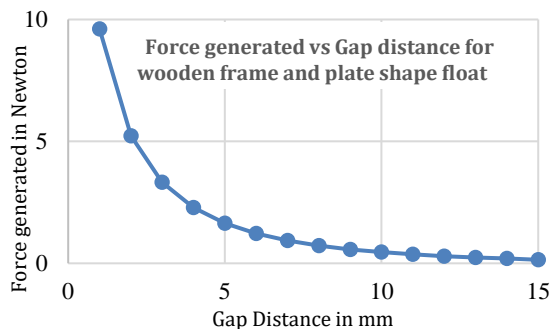


Figure 12: Amount of force for different gap distances in improved design with wooden frame, plate shape float

7. FURTHER IMPROVEMENT BY CHANGING THE SHAPE OF ELECTROMAGNET, CORE AND FLOAT

Next parameter that was changed was the core shape of electromagnet. In this case a U shape electromagnet is used with a rectangular plate type float. A rectangular float has been selected because the maximum flux density is obtained at a rectangular shape just below the electromagnet (Similar analysis of section 5). The float is a rectangular plate of dimension 60mm X 40 mm with thickness of 2.5 mm. The dimensions of electromagnet are shown in the figure. The magnetomotive force used here is 500 amp-turns. With this arrangement the flux loss will be minimum. Since the path of magnetic flux is continuous. So, there is minimum flux leakage. It is confirmed from the magnetic flux curve. From this figure we can also show that this type of electromagnet can pull a much larger weight than other combinations. It is worthy of mention that for all cases stated above ampere-turns of coil were kept constant. This is possible when flux leakage is minimized and the core has less energy storage.

7.1. Result of simulation study (U shape core)

As a consequence of this improvement, (1) highest amount of mass can be lifted with this arrangement (Figure 16) (2) Here flux leakage is least compared to other designs (Figure 14).

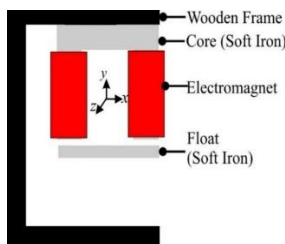


Figure 13: Schematic view of U core electromagnet

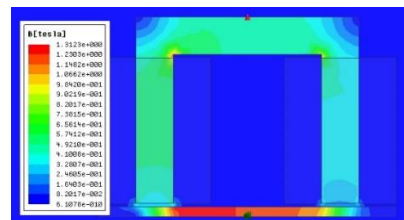


Figure 14: Simulation result of magnetic flux density with U core electromagnet

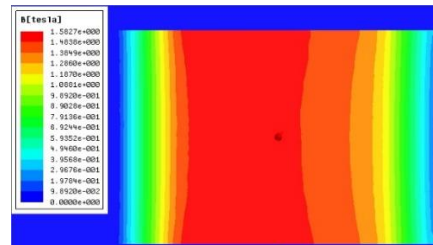


Figure 15: Simulation result of magnetic flux density with U core electromagnet on x-y plane.

(3) From figure 15, It can be concluded that plate shape rectangular is the best shape for the electromagnet, judging from its magnetic uniform flux density on the rectangular plate.

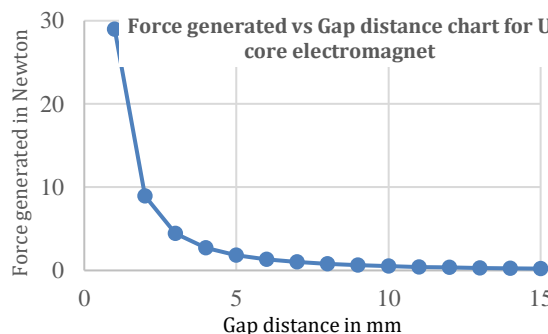


Figure 16: Comparison between previous designs vs. improved design with U core electromagnet.

(4) Also, there is no magnetic detrimental interaction between electromagnet and the frame since frame is wooden i.e. non-magnetic.

So, all the problems are solved in this design. This design is the closest to the desired ideal electromagnetic suspension system. About 3 kg mass can be lifted by this arrangement at 1mm air gap. For these reasons this design has been used in many designs to create high strength electromagnet. This also confirms the high strength of horseshoe electromagnet.

8. SUMMARY OF THE ANALYSIS FOR DIFFERENT MODELS

Table 2: Summary table of the analysis for different models.

	Models	Outcomes
1	Spherical float, circular core, wooden frame	Lots of flux leakage, force is less, flux saturation may occur in core with higher current.
2	Spherical float, circular core, iron frame	Force increases in the frame but decreases in float. Saturation of magnetic flux occurs in the frame at very low magnetomotive force. Not useful as magnetic suspension device.
3	Circular disk type float, circular core, wooden frame	Amount of force further increased than model 1, still the flux doesn't have any close loop. Flux saturation does not occur at high magnetomotive force.
4	Rectangular float, U-shape core, wooden stand	Lots of force generated, flux follow a close loop, saturation does not occur at moderate magneto-motive force. No detrimental effect between frame and electromagnet as in model 2.

For the relative advantages of model 4 this model is desired optimized design of electromagnet.

9. CONCLUSION

In this work an electromagnetic analysis is carried out for finding out an optimized model for the non -contact manipulation of magnetic materials. This paper illustrated various probable models for this purpose and the analytical results. The selection of the electromagnetic arrangement is done based on this analysis. Further experimental investigation will be carried out by using these considerations.

REFERENCES

- [1] Daniel, R., Jozsef, R. 2016. Magnetic levitation assisted aircraft take-off and landing (feasibility study – GABRIEL concept). *Progress in Aerospace Sciences*, 85 (8), 33-50.
- [2] Song, C.S., Hu, Y., Xie, S., Zhou, Z. 2012. Dynamic modeling of magnetic suspension isolator using artificial neural network: a modified genetic approach. *Journal of Vibration and Control* 19(6) 847–856.
- [3] Biswas, P.K., Bannerjee, S. 2012. Analysis of Multi-Magnet Based DC Electromagnetic Levitation System using ANSYS Simulation Software. *International Journal of Engineering, Science and Metallurgy*, 2, 618–624.
- [4] Hong, D., Member, I., Lee, K., Woo, B., Koo, D. 2008. Optimum Design of Electromagnet in Magnetic Levitation System for Contactless Delivery Application Using Response Surface Methodology. *Design*, 1–6.
- [5] Lukasz, K., Sul, P. 2015. Computer design of electromagnets. *The 4th Electronic International Interdisciplinary Conference, Electrical and Electronic engineering*, 10 (8), 211–214.
- [6] Ooshima, M., Takeuchi, C. 2011. Magnetic Suspension Performance of a Bearing less Brushless DC Motor for Small Liquid Pumps. *IEEE transactions on industry applications*, 47(1).
- [7] Dirman, H. 2010. PID Controller Design for Semi-active Car Suspension Based on Model from Intelligent System Identification. *Second International Conference on Computer Engineering and Applications*. DOI: 10.1109/ICCEA.2010.168.
- [8] Hasan, S.M., Mizuno, T., Takasaki, M., Ishino, Y. 2016. Electromagnetic analysis in magnetic suspension mechanism of a wind tunnel for spinning body. *International Journal of Applied Electromagnetics and Mechanics*, 52, 231–241. doi:10.3233/JAE-162077.

